中國機械工程學刊第四十三卷第四期第 317~326 頁(民國一百一十一年)
Journal of the Chinese Society of Mechanical Engineers, Vol.43, No.4, pp.317~326 (2022)

Optimization Design of Single Layer Honeycomb Structure under Impact Load Simulation

Chi-Lung Tsai*, Chi-Chang Hsieh**, Yung-Chang Cheng** and Huai-Chun Yeh***

Keywords：Honeycomb structure, First-order nature frequency, Uniform design, Kriging interpolation, Grey relation analysis, Entropy weighting analysis.

ABSTRACT

Based on the integrating multi-objective optimization procedure, the improve design of a honeycomb structure under the impact load and free vibration analysis is investigated in this article. Using uniform design of experiment, a group of simulation experiments is generated. Apply the finite element analysis software, the maximum displacement and first-order nature frequency of the honeycomb structure are determined for the ASTM testing and free vibration simulations, respectively. Kriging interpolation is utilized to build two surrogate models that correspond to the maximum displacement and first-order nature frequency via the numerical results in the uniform design. In order to satisfy the minimized characteristic for the maximum displacement and the maximized characteristic for the first-order nature frequency, the genetic algorithm, grey relational analysis and entropy weighting analysis are used to resolve this multi-objective optimization problem. Compared with the original design, the optimal design induces 27.33% and 15.87% improvements for ASTM D7766 testing simulation and free vibration analysis, respectively. Consequently, the stronger and demanding honeycomb structure is developed by the innovative multi-objective optimization technique.

Paper Received February, 2022. Revised April, 2022. Accepted June, 2022. Author for Correspondence: Yung-Chang Cheng

* *Graduate student: Ph. D. Program in Engineering Science and Technology, College of Engineering, National Kaohsiung University of Science and Technology, Taiwan 824, ROC.*

** *Professor, Department of Mechatronics Engineering, National Kaohsiung University of Science and Technology, Kaohsiung, Taiwan 824, ROC.*

*** *Graduate student: Department of Mechatronics Engineering, National Kaohsiung University of Science and Technology, Taiwan 824, ROC.*

INTRODUCTION

Product development in recent years has been marked by a high degree of diversity, individuality, newly invented materials, and combinations of various material kinds. Sandwich constructions with an aluminum core are extensively employed to create lightweight components in sectors like aircraft engineering and railway vehicle engineering. These sandwich honeycomb constructions are employed in engineering applications when there is a risk of high-velocity impact with light debris. (Allen, 1969)

The strength analysis of the honeycomb structure can be roughly divided into static analysis and dynamic analysis. For the static analysis, the finite element analysis of the structure strength has been investigated by the several studies (Akkus et al. 2017, Rakesh et al. 2008, Gao et al. 2011). Using compression loading, experimental and finite element methods were used by Akkus et al. (2017) to determine the mechanical behavior of aluminum honeycomb structures. Using the finite element analysis and plate theory, the static analysis of sandwich panels with a square honeycomb core is determined by Kapania et al. (2008). Applying ANSYS Workbench software, Gao et al. (2011) investigated the static analysis of the aluminum alloy honeycomb structure used in the structural design of high-speed machine tool table.

For the dynamic analysis, the finite element analysis and experiment of the structure strength have been presented by some studies. (Uğur et al., 2017; Yamashita and Gotoh, 2005; Joshilkar et al., 2018; Eloy et al. 2019) Using the ASTM D7766 standard, Uğur et al. (2017) conducted low-velocity impact load tests on honeycomb structures. Using FEM simulation and an impact experiment, Yamashita and Gotoh (2005) determined the effect of the geometry of a honeycomb cell on crush performance. Using HyperMesh and LS-DYNA, Joshilkar et al. (2018) determined the deflection and critical load for various core materials, such as copper, steel, aluminum and titanium. Applying the experiment method, Eloy et al. (2019) presented the free and forced vibrations analysis of the magnetorheological elastomer

honeycomb structure.

Besides the static and dynamic finite element analysis, the optimization design of the honeycomb structure geometry has been investigated by several literatures. (Khan et al. 2012 and Qin et al. 2019) A genetic algorithm and sequential quadratic programming was used by Khan et al. (2012) to optimize the weight of a honeycomb sandwich structure. Qin et al. (2019) used the graded thickness design method to optimize the geometrical dimensions of a hexagonal honeycomb structure with a uniform thickness.

In this study, the geometry dimensions of a honeycomb structure are optimized by the integrating optimization process. A set of simulation experiments uses a uniform design. The maximum displacement and first-order nature frequency are evaluated using ANSYS/LS-DYNA and ANASYS/Workbench software for the ASTM D7766 testing standard and free vibration analysis, respectively. Considering the grey relational analysis and entropy weighting analysis, two objective functions are combined a grey relational grade. Applying Kriging interpolation, the surrogate models is created from the results of the uniform design of experiment and the grey relational grades. A genetic algorithm is employed to resolve the multi-objective optimization problem and to determine the optimal solutions and values. Finally, the proposed multi-objective optimization procedure produces a stronger honeycomb core in a honeycomb sandwich structure.

FINITE ELEMENT ANALYSIS

Finite Element Analysis for Impact Load Simulations

Using SolidWorks software, a 3D model of a single-layer honeycomb structure is re-built. During pre-processing, the boundary conditions, elemental sizes, contact interface assumptions and appropriate material properties are defined in ANSYS/Workbench. The material for the honeycomb structure core is aluminum alloy 5052 and the material for the hammer is stainless steel. In the impact testing simulation, the deformation of the honeycomb core is the important factor after the impact load acting on the honeycomb structure. Therefore, the deformation of the honeycomb core is regarded as the main objective function to be improved. The material properties of the honeycomb core and the honeycomb structure that are relevant to the finite element analysis are shown in Table 1. (ASM 2018)

The deformation of the honeycomb core is evaluated by ANSYS/LS-DYNA software. According to ASTM D7766, the hammer of 6.35 kg is dropped on the honeycomb structure, as shown in Figure 1(a). Moreover, the contact behavior between each part is assumed bonded. To obtain a precise and accurate finite element analysis, mesh convergence analysis is executed for the honeycomb core. For the ASTM D7766 simulation, the honeycomb structure core is meshed using qualified finite elements. The convergence history for the maximum deformation is as shown in Figure 1(b). It shows that the maximum deformation will converge when the element size is smaller than 1.1 mm. Therefore, the ideal elemental size is 1.1 mm. At this element size, the maximum deformation for the ASTM D7766 simulation is 0.739 mm as shown in Figure 1(c).

Table 1: Mechanical properties of the honeycomb structural system (ASM 2018)

Part	Material	Property	Value
Honeycomb core	Aluminum Alloy 5052	Young's Modulus(Pa)	6.9×10^{10}
		Poisson's Ratio	0.3
		Density (kg/m^3)	2700
		Yield strength (MPa)	193
Hammer, Support	Stainless Steel	Young's Modulus (Pa)	1.93×10^{11}
		Poisson's Ratio	0.31
		Density (kg/m^3)	7750

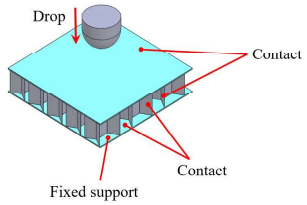

(a)

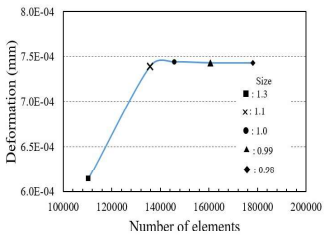

(b)

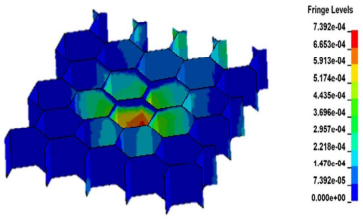

(c)

Figure 1: (a) Boundary conditions for the finite element model, (b) the maximum deformation convergent curve and (c) the deformation field for a honeycomb structure core for the ASTM D7766 damage resistance of sandwich constructions simulation.

Finite Element Analysis for Vibration Simulations

The honeycomb structure is usually applied to the floor of railway vehicles. In addition to bearing the impact loads from passengers or heavy objects, the honeycomb floor also bears the vibration signal from the bogie system. The impact loads simulation analysis has been carried out in the last section. The vibration modal analysis of the honeycomb structure is investigated in this section. In the vibration modal analysis, the 3D model of the honeycomb structure system is presented in Figure 2(a). In order to simulate the vibration behavior of the honeycomb plate used on the floor of railway vehicle, the boundary condition for the honeycomb plate is assumed to the simple support in Figure 2(a). The basically dimensions for the honeycomb core are the same as to the geometry using in the impact loads simulation.

In the finite element analysis, ANSYS/Workbench software is utilized to evaluate the natural frequencies and vibration mode. The boundary conditions setting is given as shown in Figure 2(a). In this paper, the free vibration frequency and vibration mode shape are investigated. For the vibration analysis, the honeycomb structure core is meshed using qualified finite elements. The convergence history for the nature frequency of the first vibration mode is as shown in Figure 2(b). It shows that the maximum deformation will converge when the element size is smaller than 3 mm. Therefore, the ideal elemental size is 3 mm. At this element size, the nature frequency of the first vibration mode is 1223.4 Hz as shown in Figure 2(c).

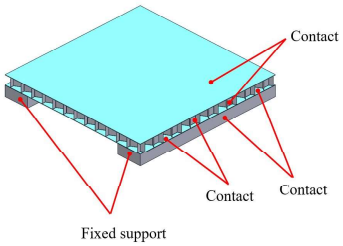

(a)

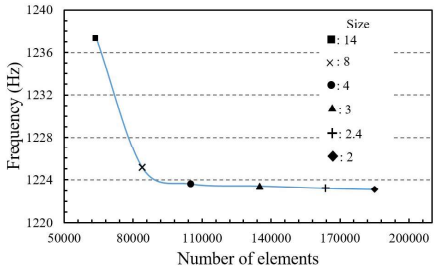

(b)

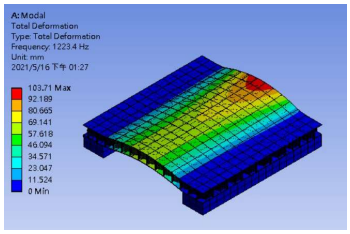

(c)

Figure 2: (a) Boundary conditions for the finite element model, (b) the nature frequency of the first vibration mode convergent curve and (c) the first-order nature frequency field for a honeycomb structure core for the free vibration analysis.

Static Analysis Validation

The static finite element analysis and experiment results are presented and compared for the honeycomb structure. The 3D testing model of the honeycomb structure is given as shown in the Figure 3(a). The material properties of this testing model is applied as Aluminum Alloy 5052. The boundary condition setting is presented in Figure 3(a). The honeycomb structure is regarded as a simple supported beam. The external load is given at the end of the honeycomb beam in Figure 3(a). Apply the ANSYS/Workbench software, the equilibrium strain is 137 mm/mm and given as shown in Figure 3(b) when the external load is 2500 g (24.5N). The element type is used as the same in the vibration analysis in the last section.

In the experiment strategy, the honeycomb structure with the same geometry dimension in Figure 3(a) is used. The honeycomb beam is clamped and the external load is given at the end as shown in Figure 4(a). The strain gauge, capacitive type transducer and HBM QuantumX MX1601B are used to measure the strain of the honeycomb beam as shown in Figure 4(b). For the HBM QuantumX MX1601B device, one 24-bit Delta Sigma A/D converter has been created in each channel. Using the strain gauges and Wheatstone bridge, the strain of the honeycomb beam can be obtained by the HBM QuantumX MX1601B device. When the external load of 2500 g is applied at the end of honeycomb beam, the numerical and experiment results is presented in Table 2. From Table 2, the difference between numerical analysis and experiment is less than 5%. Therefore, the results of the analysis using ANSYS/Workbench software are credible.

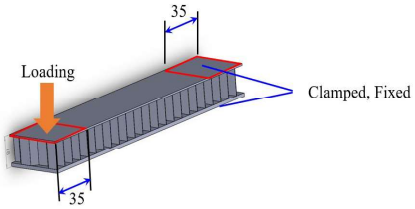

(a)

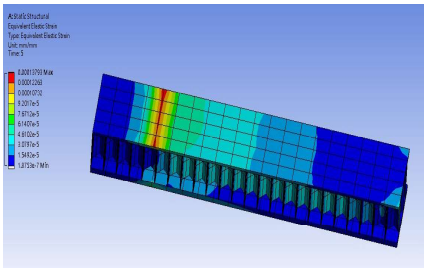

(b)

Figure 3: (a) The 3D testing model and the boundary condition setting of a honeycomb structure, (b) the equilibrium strain distribution of the honeycomb beam.

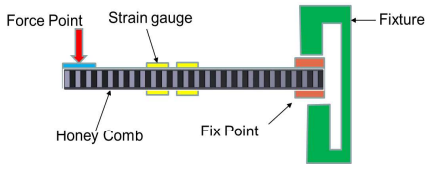

(a)

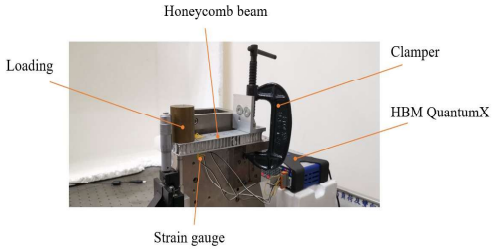

(b)

Figure 4: (a) The clamping support of a honeycomb beam, (b) the experiment devices

Table 2: Comparison of the strain from the numerical analysis and experiment

Item	Numerical results by ANSYS/Workbench (μm/m)	Experiment data (μm/m)	Error
Strain	137	135	1.48

OPTIMIZATION DESIGN ALGORITHMS

Entropy Weight Analysis

Using entropy weighting analysis the degree of uncertainty in information for probability theory is determined. Entropy weight analysis was initially developed from thermodynamics by Clausius (1865). It is widely employed in business, engineering, financial and economics and science applications. (Ayşegül and Esra, 2017; Vatansever and Akgűl, 2018; Yue, 2017) Entropy weight analysis is used to resolve multiple-criteria decision-making (MCDM) problems. Entropy weighting is an objective weighting system that uses entropy to determine the size of data. The smaller the entropy value, the smaller is the degree of disorder for the system so the entropy weight increases.

Entropy weight analysis is usually applied to determine the weight of an objective index. Four steps are used to determine the weight for a decision-making system that uses multiple criteria. (Ayşegül and Esra 2017; Vatansever and Akgűl, 2018)

Step 1. Constructing the decision matrix

A set of alternatives $\mathbf{A}=\left[A_i\right]$ compared with respect to a set of criteria $C=\left[C_j\right]$ so the $n\times m$ decision matrix $\mathbf{X}$ is evaluated as:

$$\mathrm{X}=\left[x_{ij}\right]=\begin{bmatrix} x_{11} & x_{12} & \cdots & x_{1m} \\ x_{21} & x_{22} & \cdots & x_{2m} \\ \vdots & \vdots & \ddots & \vdots \\ x_{n1} & x_{n2} & \cdots & x_{nm} \end{bmatrix} \tag{1}$$

where x_{ij} is a crisp value that represents the performance rating for each alternative A_i, with regard to each criterion C_j. The subscripts in Equation (1) are $i=1,2,\cdots,n$ and $j=1,2,\cdots,m$.

Step 2. Decision matrix normalization

To determine objective weights by measuring entropy, the decision matrix in Equation (1) is normalized for each criterion C_j as:

$$p_{ij}=\frac{x_{ij}}{\sum_{p=1}^{n} x_{pj}},\quad i=1,2,\cdots,n \tag{2}$$

The normalized decision matrix is:

$$\mathbf{P}=\left[p_{ij}\right]=\begin{bmatrix} p_{11} & p_{12} & \cdots & p_{1m} \\ p_{21} & p_{22} & \cdots & p_{2m} \\ \vdots & \vdots & \ddots & \vdots \\ p_{n1} & p_{n2} & \cdots & p_{nm} \end{bmatrix} \tag{3}$$

Step 3. Calculating entropy

The entropy value for each index is calculated as:

$$e_j=-\frac{\sum_{i=1}^{n} p_{ij}\ell n\left(p_{ij}\right)}{\ell n\left(n\right)} \tag{4}$$

where $1/\ell n(n)$ is a constant thath guarantees $0<e_j<1$.

Step 4. Calculating entropy weights

The objective entropy weights W_j for each criterion C_j are calculated as:

$$W_j=\frac{1-e_j}{\sum_{j=1}^{m}\left(1-e_j\right)} \tag{5}$$

In Equation (5), $\left(1-e_j\right)$ denotes the degree of divergence in the average intrinsic information that is contained in each criterion C_j.

Grey Relation Analysis

Based on grey system theory, grey relational analysis (GRA) was introduced by Deng (1982). GRA is used to resolve and comprehend complex issues in systems that have various variables and components. Geometrical computation is used for this analytical approach, which uses the criteria of ordinariness, regularity and totality. Grey relational analysis is used in a variety of fields (Huang and Lin, 2009 and Wang et al. 2019) to calculate the associations between reference factors and other factors for a system (Deng, 1982). The procedure for GRA is: (Huang and Lin, 2009)

Step 1. Data normalization

Before evaluating the grey relational coefficients, the input and output data must be managed. $\max_{\forall j} x_i\left(j\right)$ is the maximum value of entity j and $\min_{\forall j} x_i\left(j\right)$ is the minimum value of entity j. Three type of data processing are used:

(1) larger-the-better attributes

$$x_i^*\left(j\right)=\frac{x_i\left(j\right)-\min_{\forall j} x_i\left(j\right)}{\max_{\forall j} x_i\left(j\right)-\min_{\forall j} x_i\left(j\right)} \tag{6}$$

(2) smaller-the-better attributes

$$x_i^*\left(j\right)=\frac{\max_{\forall j} x_i\left(j\right)-x_i\left(j\right)}{\max_{\forall j} x_i\left(j\right)-\min_{\forall j} x_i\left(j\right)} \tag{7}$$

(3) nominal-the-best attributes

$$x_i^*\left(j\right)=1-\frac{\left|x_i\left(j\right)-x_{ob}\left(j\right)\right|}{max\left[\max_{\forall j} x_i\left(j\right)-x_{ob}\left(j\right),\ x_{ob}\left(j\right)-\min_{\forall j} x_i\left(j\right)\right]} \tag{8}$$

where $x_{ob}\left(j\right)$ is the objective value of entity j.

Step 2. Determining the grey relational coefficients evaluation

IF $x_0=\left[x_0\left(1\right),x_0\left(2\right),\cdots,x_0\left(j\right),\cdots,x_0\left(k\right)\right]$ is the referential series with k entities of $x_1,x_2,\cdots,x_N$,then, $x_i=\left[x_i\left(1\right),x_i\left(2\right),\cdots,x_i\left(j\right),\cdots,x_i\left(k\right)\right]$.

The grey relational coefficient $\gamma_{0i}\left(j\right)$ between the series x_i and the referential series x_0 at the j-the entity is defined as:

$$\gamma_{0i}\left(j\right)=\frac{\Delta\min+\Delta\max}{\Delta_{0i}\left(j\right)+\Delta\max} \tag{9}$$

where, $\Delta_{0i}\left(j\right)=\left|x_0\left(j\right)-x_i\left(j\right)\right|$, $\Delta\max=\max_{\forall j}\max_{\forall j}\Delta_{0i}\left(j\right)$, $\Delta\min=\min_{\forall j}\min_{\forall j}\Delta_{0i}\left(j\right)$.

Step 3. Calculating the grey relational grade

The grey relation coefficients, $\gamma_{0i}\left(j\right)$ are determined at Step 2 and the grey relational grade for a series of x_i is written as:

$$\Gamma_{0i}=\sum_{j=1}^{k} W_j\gamma_{0i}\left(j\right) \tag{10}$$

where, W_j is the weight of attribute j. This is dependent on the judgment of decision-makers or the geometry of the research structure. The sum of all weights equals one. For this study, the weight, W_j, is calculated from the entropy weight analysis. The entropy weight analysis is detailed in the last section

Kriging Interpolation

A surrogate model is used to present the compendium formula for the relationship between input and output information. It is governed by statistical regression, Bayesian networks, a radial basis function or Kriging interpolation. If noise factors are included in the system, Kriging interpolation is used to make an initial estimate and is widely employed in a variety of engineering research fields. (Bouhlel et al., 2018 and Asa et al., 2012) This study uses Kriging interpolation to generate a proxy model of the target function using the unique experimental points from the uniform design outcomes.

The Kriging surrogate model $\hat{y}_m\left(\boldsymbol{x}\right)$ for the objective function is derived using a zero-order regression function and a Gaussian correlation function:

$$\hat{y}_{\mathrm{m}}\left(\boldsymbol{x}\right)=\beta+\boldsymbol{r}^T\left(\boldsymbol{x}\right)\mathbf{R}^{-1}\left(\boldsymbol{Y}-\boldsymbol{G}\beta\right) \tag{11}$$

where $\boldsymbol{x}=\{x_1,x_2,\ldots,x_p\}$ denotes a vector that consists of unknown input variables and p is the number of unknown variables, $\boldsymbol{r}\left(\boldsymbol{x}\right)$ specifies a vector of length n and is a function of the unknown input variables, $\boldsymbol{Y}=\{y_1,y_2,\ldots,y_n\}^T$ denotes a known response vector for an unknown function, $\boldsymbol{G}$ denotes a n-dimensional column vector that is filled with ones, $\mathbf{R}=\left[R_{ij}\right]_{n\times n}$ specifies a known square matrix and denotes an identified constant. More detailed descriptions can be found in Cheng et al. (2019).

IMPROVEMENT DESIGN OF THE HONEYCOMB STRUCTURE

Uniform Design Of Experiment

The four parameters for the honeycomb structure

that significantly affect the experimental indices are the system control factors to be improved. The main design parameters for the honeycomb structure are shown in Figure 5. The first control factor, which is denoted as D, is the diameter of the inscribed circle of the honeycomb core. The second control factor, which is denoted as T, is the thickness of the honeycomb core. The third control factor, which is denoted as H, is the height of the honeycomb core. The fourth control factor, which is denoted as TT, is the thickness of the stainless steel plate. For each system control factor, the code numbers for each part and the upper and lower limits are shown in Table 3.

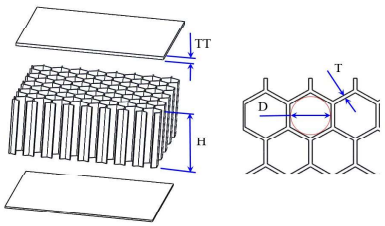

Figure 5: Four system control factors for the honeycomb structure model

Table 3. The lower and upper bounds and the basic values for four system control factors

System control factor	Notation	Lower bound (mm)	Basic value (mm)	Upper bound (mm)
Diameter of the inscribed circle of the honeycomb core	D	17	21	25
Thickness of the honeycomb core	T	0.05	0.06	0.1
Height of the honeycomb core	H	15	20	25
Thickness of the stainless steel plate	TT	0.8	1	1.2

Because of continuity for the control factors, the design space can be regarded as a continuous space. Hence, uniform design of experiment method constructed from Fang and Wang (1994) is utilized to build a group of sample points that are dissipated constantly in the uninterrupted design space. According to the characteristic of the uniform design of experiment method, this uniform design is broadly employed in many engineering areas. (Li et al., 2017; Li and Yang, 2019; Chatterjee et al., 2017)

Based on the uniform design of the experiment (Fang and Wang, 1994) and considering restrictions in machine instrumentation, each factor is simply separated into 16 levels, and 16 simulation tests are created using a uniform table . Table 4 shows the experimental levels and bounds for each control component, the experiments are arranged as shown in Table 4(a). Using SolidWorks software, the 3D geometric model is created for a specific design of honeycomb structure for each simulation experiment. Applying the FEA method by ANSYS/LS-DYNA and ANSYS/Workbench software, for each experimental simulation, the maximum displacement and first-order nature frequency of the honeycomb core and structure has been determined and is listed in Table 4(a).

In Table 4, YD denotes the maximum displacement for the honeycomb core for the ASTM D7766 damage resistance of sandwich constructions simulation, YF denotes the first-order nature frequency for the honeycomb structure for the free vibration simulation. From the simulation results given in Table 4(a), the improvement rate compared with the original design for each experiment simulation has been calculated and presented in Table 4(b). From Table 4, the maximum displacement for ASTM D7766 testing simulation decreases to 0.498 mm in the 14th experiment. The maximum first-order nature frequency for free vibration increases to 1482.1 Hz in the 13th experiment. In Table 4(b), the 2nd experiment has two positive improvements for YD and YF. Therefore, the design in the 2nd experiment is regarded to the improved design in the uniform design of experiment strategy. Although the positive improvements for YD and YF are appeared in the 2nd experiment, the improvement rates are not the highest in all simulation experiments. So, the problem must be solved using the multi-objective optimization method that is described in the following.

Table 4: The uniform experiments and results for the uniform table $U_{16}^{*}\left(16^{12}\right)$

(a)

No.	D (mm)	T (mm)	H (mm)	TT (mm)	YD (mm)	YF (Hz)
1	17.00	0.063	18.33	0.99	0.824	1254.2
2	17.53	0.080	22.33	1.20	0.550	1405.2
3	18.07	0.097	15.00	0.96	0.954	754.5
4	18.60	0.057	19.00	1.17	0.633	1161.5
5	19.13	0.073	23.00	0.93	0.727	1480.8
6	19.67	0.090	15.67	1.15	0.896	1241.9
7	20.20	0.050	19.67	0.91	0.670	1177.6
8	20.73	0.067	23.67	1.12	0.563	856.5
9	21.27	0.083	16.33	0.88	0.984	1264.9
10	21.80	0.100	20.33	1.09	0.864	1439.6
11	22.33	0.060	24.33	0.85	0.591	861.4
12	22.87	0.077	17.00	1.07	0.871	1179.8
13	23.40	0.093	21.00	0.83	1.028	1482.1
14	23.93	0.053	25.00	1.04	0.498	952.87
15	24.47	0.070	17.67	0.80	0.830	1216.6
16	25.00	0.087	21.67	1.01	0.837	1220.6

(b)

Experiment No.	Improvement of YD (%)	Improvement of YF (%)
1	2.52	-11.42
2	14.86	25.54
3	-38.33	-29.10
4	-5.06	14.41
5	21.04	1.70
6	1.51	-21.19
7	-3.74	9.42
8	-29.99	23.86
9	3.39	-33.17
10	17.67	-16.84
11	-29.59	20.09
12	-3.56	-17.86
13	21.15	-39.07
14	-22.11	32.62
15	-0.56	-12.22
16	-0.23	-13.27

OPTIMAL DESIGN PROCEDURE AND RESULTS

This study uses a uniform design of experiment, Kriging interpolation, grey relational analysis, entropy weighting analysis and a genetic algorithm to solve a multi-objective optimization design problem. The optimization design procedure is shown in Figure 6. The detailed description and results are presented in the following.

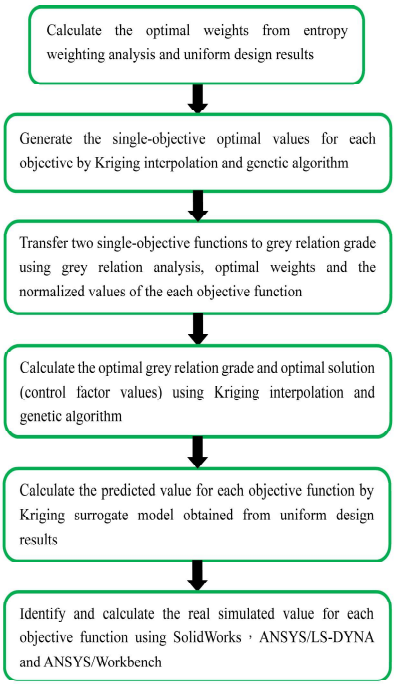

Figure 6: Multi-optimization design process

Step 1. Using entropy weighting analysis and the uniform design results, determine the appropriate weights.

According to the numerical results in Table 4(a) and 4(b), the optimal weight for each objective function using entropy weight analysis is (0.5744, 0.4256).

Step 2. Create a Kriging surrogate model using Kriging interpolation and use a genetic algorithm to determine the optimal design parameters for a single objective.

The Kriging surrogate model for each objective function is developed using Kriging interpolation and the results of the uniform design in Table 4. The single-objective optimal design values are obtained using a genetic algorithm, as shown in Table 5.

Table 5. Optimal value of the single-objective optimization design

Objective function	YD (mm)	YF (Hz)
Optimal value	0.466	1577.7

Step 3. Two single objective functions are translated to grey relational grades using grey relational analysis and the optimal weights and normalized values for each objective function.

The results for the uniform design in Table 4(a) are normalized for each objective function using the optimal value in Table 5. Grey relation analysis using Equations (6)-(10) and the optimal weights from Step 1 to determine the grey relational grade. The two single objective functions are combined into one grey relational grade objective function. Table 6 shows the grey relational grade for each experiment.

Table 6: Results for the grey relational grade

Experiment No.	Grey relational grade
1	0.568
2	0.820
3	0.423
4	0.622
5	0.728
6	0.547
7	0.602
8	0.625
9	0.541
10	0.655
11	0.591
12	0.530
13	0.660

14	0.779
15	0.553
16	0.552

Step 4. Using Kriging interpolation and a genetic algorithm, calculate the optimal grey relational grade and the optimal solution (control factor values).

Kriging interpolation is used to create a surrogate model for the grey relational grade. Using a genetic method, the optimal grey relational grade and the optimal solution are determined, as shown in Table 7. The optimal solution is the optimal geometric dimensions for the honeycomb structure. The optimal grey relational grade is 0.8211, which is greater than all of the grey relation grades in Table 6.

Table 7: Optimal solution and the grey relational grade

Optimal solution (Optimal dimension of the honeycomb structure)				Optimal grey relational grade
D (mm)	T (mm)	H (mm)	TT (mm)	
17.97	0.078	22.97	1.20	0.8211

Step 5. Using the Kriging model that is derived from the results of the uniform results, the predicted value for each objective function is calculated.

The predicted optimal values for each objective function using the optimal grey relational grade, optimal entropy weights, and the Kriging surrogate model for each objective function are given in Table 8.

Step 6. Using SolidWorks, ANSYS/LS-DYNA and ANSYS/Workbench, the real simulated value for each objective function is calculated.

The optimal honeycomb structure model is reconstructed using SolidWorks software. Using ANSYS/LS-DYNA and ANSYS/Workbench software, the true displacement and first-order nature frequency are calculated. Table 8 shows the predicted error for YD and YF. The predicted errors for YD and YF are 0.19 %, and 0.03 %. All of the predicted errors are less than 3 % so the optimization procedure is complete. The displacement and first-order nature frequency in the final design are shown in Figures 7.

The values of the maximum displacement and first-order nature frequency for various phases are shown in Table 9. After the uniform design of experiment, the maximum displacement for YD decreases to 0.55 mm, the first-order nature frequency for YF increases to 1405.2 Hz. The improvements in YD, and YF are 25.54 % and 14.86 %, respectively. After executing the multi-objective optimization, the maximum displacement for YD decreases to 0.537 mm, the first-order nature frequency for YF increases to 1417.5 Hz. The improvements for YD and YF are 27.33 % and 15.87 %, respectively. All of the values for the displacement and first-order nature frequency are improved successfully.

Table 8: Optimal predicted value and predicted error

Measure	Predicted value	Real value	Predicted Error (%)
YD (mm)	0.538	0.537	0.19
YF (Hz)	1417.9	1417.5	0.03

Table 9: Values and improvement in measures for different phases

Phase	Measure	Value	Improvement (%)
Original design	YD (mm)	0.739	—
	YF (Hz)	1223.4	—
After uniform experiments	YD (mm)	0.550	25.54
	YF (Hz)	1405.2	14.86
After multi-objective optimization	YD (mm)	0.537	27.33
	YF (Hz)	1417.5	15.87

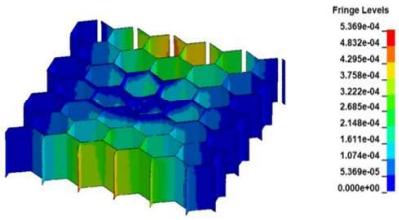

(a)

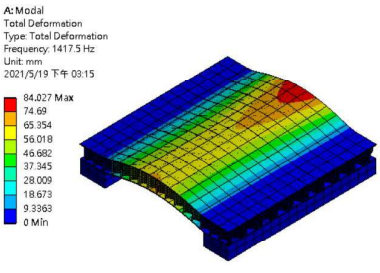

(b)

Figure 7: The distribution of (a) the displacement for ASTM D7766 testing standard and (b) first-order nature frequency for free vibration analysis in the final optimal design.

CONCLUSION

This study involves an analysis of the honeycomb core in the honeycomb structure. The design of each of the parameters is planned using a uniform design of experiment. The finite element software, ANSYS/LS-DYNA and ANSYS/Workbench, are utilized to evaluate the distribution of the displacement in the honeycomb

core for ASTM D7766 standard simulation, and the nature frequency for the free vibration analysis. The strategy for improvement uses a uniform design of experiment to create the experimental data, the displacement and first-order nature frequency for the honeycomb structure. After the uniform design of experiment, the improvement in the maximum displacement and first-order nature frequency is 25.54 % and 14.86 %. After the multi-objective optimization process, the final respective improvement in the maximum displacement and first-order nature frequency is 27.33 % and 15.87 %. From the final optimization results, the maximum displacement of the honeycomb core has been reduced. Moreover, the first-order nature frequency has been increased. As a result, this article produces an improved design for the honeycomb core in the honeycomb structure.

ACKNOWLEDGEMENTS

The authors gratefully acknowledge the financial support of the Ministry of Science and Technology (MOST) under grant no's. 109-2221-E-992-022 and 110-2221-E-992 -069. Thanks for the technical support of the TCcore Applied Honeycomb Technology Company.

REFERENCES

Akkus H., Duzcukoglu H. and Sahin O. S., "Experimental research and use of finite elements method on mechanical behaviors of honeycomb structures assembled with epoxy-based adhesives reinforced with nanoparticles,"; Journal of Mechanical Science and Technology, Vol. 31, pp. 165-170 (2017).

Allen G. 1969. Analysis and Design of Structural Sandwich Panel. England: Pergamon Press Oxford.

Asa E., Saafi M., Membah J. and Billa A., "Comparison of Linear and Nonlinear Kriging Methods for Characterization and Interpolation of Soil Data,"; Journal of Computing in Civil Engineering, Vol. 26, No. 1, pp. 11-18 (2012).

ASM Aerospace Specification Metals Inc. 2018: Aluminum 5052-H38.
http://asm.matweb.com/search/SpecificMaterial.asp?bassnum=MA5052H38.

ASM Aerospace Specification Metals Inc. 2018: AISI Type 302 Stainless Steel.
http://asm.matweb.com/search/SpecificMaterial.asp?bassnum=MQ302AC.

ASTM International. 2016. ASTM D7766: Standard Practice for Damage Resistance Testing of Sandwich Constructions.

Ayşegül T. I. and Esra A. A., "The decision-making approach based on the combination of entropy and rov methods for the apple selection problem,"; European Journal of Interdisciplinary Studies, Vol. 3, No. 3, pp. 80-86 (2017).

Bouhlel M. A., Bartoli N., Regis R. G., Otsmane A. and Morlier J., "Efficient Global Optimization for High-Dimensional Constrained Problems by using the Kriging Models Combined with the Partial Least Squares Method,"; Engineering Optimization, Vol. 50, No. 12, pp. 2038-2053 (2018).

Chatterjee K., Ou Z., Phoa F. K. H. and Qin H., "Uniform Four-Level Designs from Two-Level Designs: a New Look,"; Statistica Sinica, Vol. 27, pp. 171-186 (2017).

Cheng Y. C., Jiang C. P. and Lin D. H., "Finite Element based Optimization Design for a One-Piece Zirconia Ceramic Dental Implant under Dynamic Loading and Fatigue Life Validation,"; Structural and Multidisciplinary Optimization, Vol. 59, No. 3, pp. 835-849 (2019).

Clausius R., "Ueber verschiedene für die Anwendung bequeme formen der Hauptgleichungen der mechanischen Wärmetheorie."; Annalen der Physik, Vol. 201, No. 7, pp. 353–400 (1865).

Deng J., "Control problems of grey systems,"; Systems and Control Letters, Vol. 1, pp. 288–294 (1982).

Eloy F. S., Gomes G. F., Ancelotti A. C., Cunha S. S., Bombard A. J. F. and Junqueira D. M., "A numerical-experimental dynamic analysis of composite sandwich beam with magnetorheological elastomer honeycomb core,"; Composite Structures, Vol. 209, pp. 242-257 (2019).

Fang K. T. and Wang Y., Number-Theoretic Methods in Statistics. London: Chapman & Hall (1994).

Gao D. Q., Zhang F., Mao Z. Y., Lin H. and Yi J. M., "Application of Honeycomb Structure in Machine Tool Table,"; Advanced Materials Research, Vol. 308-310, pp. 1233-1237 (2011).

Huang Y. L. and Lin C. T., "Constructing grey relation analysis model evaluation of tourism competitiveness,"; Journal of Information and Optimization Sciences, Vol. 30, No. 6, pp. 1129-1138 (2009).

Joshilkar P., Deshpande R. D. and Kulkarni. R. B., "Analysis of honeycomb structure,"; International Journal for Research in Applied Science and Engineering Technology, Vol. 6, No. V, pp. 950-958 (2018).

Kapania R. K., Soliman H. E., Vasudeva S., Hughes O. and Makhecha D. P., "Static Analysis of Sandwich Panels with Square Honeycomb Core,"; AIAA Journal, Vol. 46, No. 3, pp. 627-634 (2008).

Khan H. A., Vance F. H., Israr A. and Rehman T. U., "An integrated approach for optimization of honeycomb sandwich structure under impact load,"; Applied Mechanics and Materials, Vol. 152-154, pp. 1717-1722 (2012).

Li B., Wang W., Zhang X., Zhang D., Mu W. and Liu F., “Integrating Uniform Design and Response Surface Methodology to Optimize Thiacloprid Suspension,”; Scientific Reports, Vol. 7, No. 1, pp. 1-9 (2017).

Li T. Z. and Yang X. L., “An Efficient Uniform Design for Kriging-Based Response Surface Method and its Application,”; Computers and Geotechnics, Vol. 109, pp. 12-22 (2019).

Qin R., Zhou J. and Chen B., “Crashworthiness design and multiobjective optimization for hexagon honeycomb structure with functionally graded thickness,”; Advances in Materials Science and Engineering, Vol. 2019, Article ID 8938696, pp.1-13, (2019).

Uğur L., Duzcukoglu H., Sahin O. S. and Akkuş. H., “Investigation of impact force on aluminium honeycomb structures by finite element analysis,”; Journal of Sandwich Structures and Materials, Vol. 22, No. 1, pp. 87-103 (2020).

Vatansever K. and Akgűl Y., “Performance evaluation of websites using entropy and grey relational analysis methods: the case of airline companies,”; Decision Science Letters, Vol. 7, pp. 119–130 (2018).

Wang L., Yin K., Cao Y. and Li X., “ A new grey relational analysis model based on the characteristic of inscribed core (IC-GRA) and its application on seven-pilot carbon trading markets of china,”; International Journal of Environmental Research and Public Health, Vol. 16, No. 1, pp. 99-1~99-16 (2019).

Yamashita M. and Gotoh M., “Impact behaviour of honeycomb structures with various cell specifications numerical simulation and experiment.”; International Journal of Impact Engineering, Vol. 32, No. 1-4, pp. 618–630 (2005).

Yue C., “Entropy-based weights on decision makers in group decision-making setting with hybrid preference representations,”; Applied Soft Computing, Vol. 60, pp. 737–749 (2017).

單層蜂巢結構在衝擊力作用下的最佳設計

蔡騏隆 謝其昌 鄭永長 葉懷鈞
國立高雄科技大學 機電工程系

摘 要

根據多目標最佳化程序，本文研究了衝擊載荷和自由振動分析下的蜂巢結構改善設計。採用均勻實驗設計，建立一組模擬實驗。應用有限元分析軟體，分別為ASTM測試和自由振動模擬，計算蜂巢結構的最大位移和一階自然頻率。採用Kriging插值法，通過均勻設計中的數值結果，建立對應於最大位移和一階自然頻率的代理模型。為了滿足最大位移的最小化特性和一階自然頻率的最大化特性，採用基因算法、灰關聯分析和熵權分析來求解該多目標最佳化問題。與原始設計相比，最佳化設計在 ASTM D7766 測試模擬和自由振動分析方面分別提高了 27.33% 和 15.87%。因此，透過創新的多目標最佳化技術開發了更堅固和要求更高的蜂巢結構。